Florence, Italy 12-16 July 2015
ICSV22
The 22nd International Congress on Sound and Vibration

A GENERALISED FFOWCS-WILLIAMS AND HAWKINGS FORMULATION APPLIED TO FLOW SIMULATIONS WITH VORTICAL OUTFLOW

S. Sinayoko, M. C. M. Wright, R. D. Sandberg
University of Southampton, Highfield, Southampton SO17 1BJ, United Kingdom
email: s.sinayoko@soton.ac.uk

The FW-H equations allow to extrapolate acoustic fluctuations outside of a particular surface. In many applications, such as jet noise or turbomachinary noise, parts of the surface may lie in regions of high vorticity. Vorticity crossing the surface generates spurious noise sources in the thickness and loading terms. These sources are cancelled out by the quadrupole sources outside of the surface. Unfortunately, these quadrupole sources are usually neglected which leads to incorrect noise predictions. A generalized form of the FW-H formulation was recently developed to overcome this problem. It relies on a distributed extrapolation zone, instead of a single surface. This paper applies this new theory to the simplified problem of a divergence-free Gaussian vortex crossing a spherical FW-H surface. It is shown that the two key parameters driving the accuracy of the noise prediction are the distance between two outflow surfaces, which should be bigger than the characteristic length of the vortex, and the thickness of the outflow region, which should be small compared to the acoustic wavelength. Reductions in the sound pressure level of the spurious noise of up to 13 dB are obtained using 4 surfaces.

1. Introduction

The Ffowcs-Williams and Hawkings (FW-H) equations [13] show that acoustic radiation from a given volume of fluid is equivalent to that generated in a quiescent medium by a distribution of monopoles, dipoles and quadrupole sources on a (usually) closed surface, and have been widely used to extrapolate acoustic fields from unsteady flow simulations. In several applications, such as jet noise [9, 11, 5, 2], rotor noise [3] or airfoil noise [14], it can be expensive or unavoidable to place the extrapolation surface so that it contains all the vortical regions of the flow. However, vorticity crossing the extrapolation surface can cause spurious acoustic sources when the quadrupoles that constitute the volume sources are neglected for reasons of computational efficiency. These spurious sources can damage the accuracy of the noise predictions. Allowing extrapolation surfaces to be placed closer to the regions of the flow that generate true acoustic radiation would reduce the computational cost of noise prediction.

The first solution to this problem was proposed by Wang et al. [12] and relies on estimating the contribution from the volume sources from Lighthill's acoustic analogy and the assumption of frozen turbulence. This idea was extended by Avital et al. [1] to allow for a non-uniform convection velocity, and by Ikeda et al. [4] and Nitzkorski et al. [7] by using the FW-H equations instead of Lighthill's

equation. Unfortunately, the hypothesis of frozen turbulence is not always applicable so there is a need for alternative solutions.

An alternative technique that appears equally effective was proposed by Shur et al. [9]. It consists in estimating the contribution from the outflow surface by averaging over multiple outflow surfaces separated by an appropriately chosen distance. This technique was applied successfully to jet noise[11]. A detailed study of that approach for predicting jet noise was carried out by Mendez et al. [5] who reported the frequency range over which spurious noise is reduced for a given separation distance between surfaces and a given number of surfaces. The distance between surfaces defines the maximum frequency for noise cancellation. The number of surfaces times the distance between each surface defines the minimum frequency of noise cancellation.

Wright et al. [15] recently proposed a generalization of the FW-H equations that replaces the extrapolation surface with a distributed zone in order to reduce the intensity of these spurious vorticity-related acoustic sources. A special case of this generalization corresponds to averaging over multiple surfaces [9, 5], discussed in the previous paragraph. The advantage of this new approach is that it provides more flexibility in controlling the spurious noise from the outflow boundary. However, this new approach has yet to be applied to numerical data so it remains to be seen whether it will prove more effective than current approaches.

This paper will investigate the spurious noise due to a convecting vortex crossing the outflow boundary in a uniform flow, by using the generalized FW-H equations of Wright et al. [15]. The objective will be to obtain guiding principles for choosing the number of surfaces and the distance between each surface. Section 2 presents a generalized version of Wright et al. 's FW-H equations with a distributed outflow region that accounts for the presence of a uniform flow. In section 3, the formulation is applied to the case of a 3D vortex convecting downstream and crossing the porous surface.

2. Theory

2.1 Windowed acoustic analogy in a uniform flow

Wright at al [15] derive the general form of a windowed acousic analogy in a quiescent medium. Since we would like to allow for the presence of a co-flow, this paper starts from the Ffowcs-Williams and Hawkings equations in a uniform medium, as derived by Najafi-Yazdi et al. [6]. For a window $W(f)$, and a stationary extrapolation region $0 < f < 1$, one can write

$$\left(\frac{D}{Dt} - \nabla^2\right) c_0^2(\rho - \rho_0) = \frac{D}{Dt}[Q_i n_i W'(f)] - \frac{\partial}{\partial x_i}[L_{ij} n_j W'(f)] + \frac{\partial^2}{\partial x_i \partial x_j}[T_{ij} W(f)], \tag{1}$$

where

$$Q_i = \rho(u_i + U_{0i}), \tag{2}$$

$$L_{ij} = \rho u_i (u_j + U_{0j}) + (p - p_0)\delta_{ij} - \sigma_{ij}, \tag{3}$$

$$T_{ij} = \rho u_i u_j + [(p - p_0) - c_0^2(\rho - \rho_0)]\delta_{ij} - \sigma_{ij}, \tag{4}$$

with ρ the density field, p the pressure field, u_i the unsteady velocity field, U_{0i} the mean velocity field, σ_{ij} the viscous stress tensor.

We shall assume that the windowing function takes the form

$$W(f) = \sum_{i=1}^{N} a_i H(f - f_i), \quad \sum_{i=1}^{N} a_i = 1, \tag{5}$$

where $f_{i+1} > f_i$ for all i. We also have

$$W'(f) = \sum_{i=1}^{N} a_i \delta(f - f_i). \tag{6}$$

Following Najafi-Yazdi et al.'s [6] derivation of formulation 1C for a stationary surface and a stationary observer ("wind tunnel" case), the unsteady pressure is given by

$$4\pi(p-p_0) = \sum_{n=1}^{N} a_n \int_{f_i=0} \left\{ \left[(1-M_0\tilde{R}_i)\frac{\dot{Q}_i n_i}{R^*} - U_0 \tilde{R}^*_z \frac{Q_i n_i}{R^{*2}} \right]_{\tau_e} + \left[\frac{\dot{L}_{ij} n_j \tilde{R}_i}{c_0 R^*} + \frac{L_{ij} n_j \tilde{R}^*_i}{R^{*2}} \right]_{\tau_e} \right\} \mathrm{d}\boldsymbol{\eta}, \tag{7}$$

where

$$R^* = \sqrt{\beta^2[(x_o-x_s)^2 + (y_o-y_s)^2] + (z_o-z_s)^2}, \tag{8}$$

$$R = \frac{-M(z_o-z_s) + R^*}{\beta^2} \tag{9}$$

$$\tilde{R}_1 = \frac{x_o-x_s}{\beta^2} \qquad \tilde{R}_2 = \frac{y_o-y_s}{\beta^2} \qquad \tilde{R}_3 = \frac{-M+\tilde{R}^*_z}{\beta^2} \tag{10}$$

$$\tilde{R}^*_1 = \beta^2 \frac{x_o-x_s}{R^*} \qquad \tilde{R}^*_2 = \beta^2 \frac{y_o-y_s}{R^*} \qquad \tilde{R}^*_3 = \frac{z_o-z_s}{R^*}. \tag{11}$$

The above expression neglects the quadrupole sources. If the extrapolation region is free of vorticity fluctuations, then each surface yields the same pressure field and the above formula reduces to formulation 1C:

$$4\pi(p-p_0) = \int_{f_i=0} \left\{ \left[(1-M_0\tilde{R}_i)\frac{\dot{Q}_i n_i}{R^*} - U_0 \tilde{R}^*_z \frac{Q_i n_i}{R^{*2}} \right]_{\tau_e} + \left[\frac{\dot{L}_{ij} n_j \tilde{R}_i}{c_0 R^*} + \frac{L_{ij} n_j \tilde{R}^*_i}{R^{*2}} \right]_{\tau_e} \right\} \mathrm{d}\boldsymbol{\eta}. \tag{12}$$

If the extrapolation surface $f_i = 0$ intersects a vortical region of the flow field, it will generate some spurious noise. That noise would be cancelled were the quadrupole sources taken into account. The hope is that the extrapolation region and the coefficients $(a_i)_{1\le i\le N}$ can be chosen in such a way as to minimize the spurious noise.

3. Results and discussion

3.1 Validation

The formulation 1C of equation (12) is implemented in Python using the NumPy library. The code is validated by comparing the FW-H solution with an analytical solution, for a monopole source and a dipole source. In both cases, the point souce is located at the origin of the Cartesian coordinate system x_i and the FW-H surface is a cube of side r_0. Each face of the cube is discretized into m uniform cells, where m must be such that the Helmholtz number $\mathrm{He} = kr_0/(m\beta) \le 1$, so that the retarded time can be considered constant over each cell, i.e. the cell is compact. The integral is carried out by summing the contribution from each cell, where we have used a minimum of 8 cells along each edge, so that m is defined for a given Helmholtz number as

$$m \equiv \max(8, \mathrm{ceil}(kr_0/(\mathrm{He}\beta))). \tag{13}$$

The cube edge size is either $r_0 = \lambda/100$ (compact case) or $r_0 = \lambda$ (non-compact case). We have used either a low Mach number $M = 0.2$ or a high Mach number $M = 0.9$.

For the monopole source and a dipole source, the velocity potential was defined respectively as ϕ'_m and ϕ'_d, where

$$\phi'_m = \frac{A}{4\pi R^*} e^{i\omega t}, \qquad \phi'_d = \frac{\partial}{\partial x_o}\left(\frac{A}{4\pi R^*} e^{i\omega t} \right), \tag{14}$$

so the dipole was aligned with the x-axis, in the cross-flow direction.

The source terms in equation (12) are linearlized and the pressure, the fluctuating parts of the density and velocity fields are given by

$$p' = -\rho_0 \left(\frac{\partial}{\partial t} + U \frac{\partial}{\partial z} \right) \phi', \qquad \rho' = p'/c_0^2, \qquad \boldsymbol{u}' = \boldsymbol{\nabla} \phi. \tag{15}$$

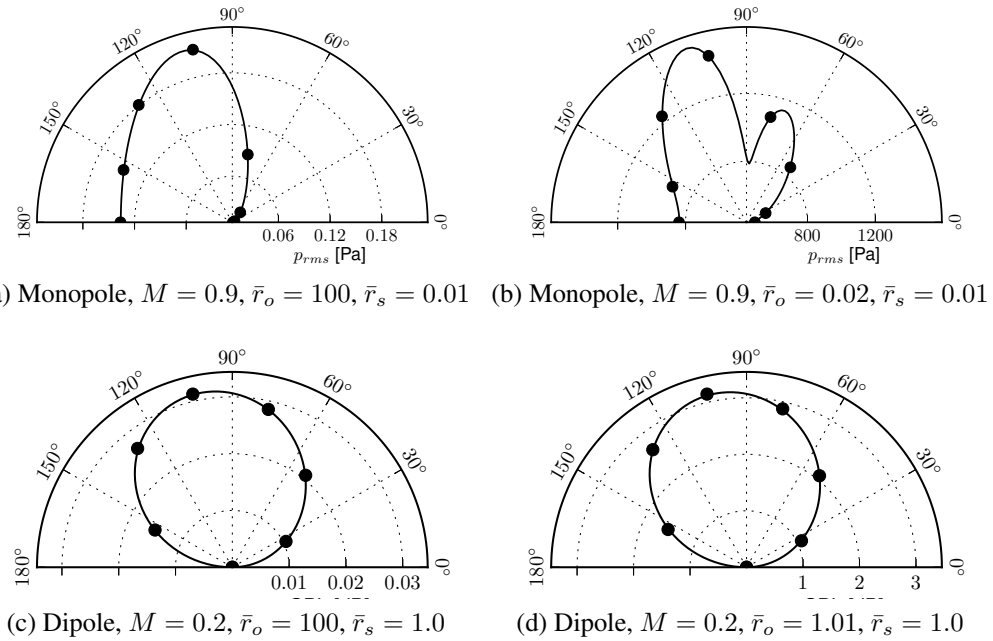

(a) Monopole, $M = 0.9$, $\bar{r}_o = 100$, $\bar{r}_s = 0.01$ (b) Monopole, $M = 0.9$, $\bar{r}_o = 0.02$, $\bar{r}_s = 0.01$

(c) Dipole, $M = 0.2$, $\bar{r}_o = 100$, $\bar{r}_s = 1.0$ (d) Dipole, $M = 0.2$, $\bar{r}_o = 1.01$, $\bar{r}_s = 1.0$

Figure 1: Validation of FW-H formulation 1C [6] at frequency $f = 50$Hz using a monopole source in a uniform flow of Mach $M = 0.9$ (top row) or a dipole source at Mach $M = 0.2$ (bottom row). The observer distance is $r_o = \lambda \bar{r}_o$: the observer is in the far field (left column) or in the near field (right column) relative to the surface. The FW-H surface is a cube of side $r_s = \lambda \bar{r}_s$: it is either compact (top row) or non-compact (bottom row). Lines denote exact solution, the dots the current FW-H results.

The results are shown in figure 1 for a variety of configurations: a monopole source (top row) or a dipole source (bottom row) at frequency $f = 50$Hz, with an observer in the far field (left column) or in the near field (right column) relative to the porous surface. The observer distance is defined relative to the acoustic wavelength as $r_0 = 100\lambda$ in the far field, and $r_0 = r_s + 0.01\lambda$ in the near field. The distance r_s defines the location of the porous surface from the origin. The surface is compact in the top row ($r_s = 0.01\lambda$) and non-compact ($r_s = \lambda$) in the bottom row. Finally, the sources are placed in a uniform flow at high Mach number (top row, $M = 0.9$) or low Mach number (bottom row, $M = 0.2$). In all cases, the dots represent the FW-H solution, and the solid line the exact solution.

The results were obtained by assuming He $= 1.0$ and by defining the number of cells along the edges of the square FW-H surfaces from equation (13). The FW-H solutions agree with the exact solution to within 0.2 dB. Similar results were obtained at high frequency $f = 5$kHz. These results validate the formulation and implementation of equation (12).

3.2 Convecting vortex

Methodology

We investigate the sound due to a divergence-free Gaussian vortex convecting with the flow, originating from the origin and crossing the outlet FW-H surfaces.

The vortex is defined based on a vector potential, as was proposed by Sescu and Hixon [8]:

$$\boldsymbol{u} - \boldsymbol{u}_0 = \boldsymbol{\nabla} \times \boldsymbol{\Psi}, \qquad \Psi_i(\boldsymbol{x}, t) = A_i U \exp\left\{-[x^2 + y^2 + (z - U_0 t)^2]/(2\sigma^2)\right\}, \tag{16}$$

where A_i is defined as the strength of the vortex in the i-direction. The vortex generates 3D velocity fluctuations but no density or pressure fluctuations. In this paper, the amplitude is the same in all directions and is set to $A_i = 0.1$. The instantaneous velocity field of this vortex is illustrated in figure 2.

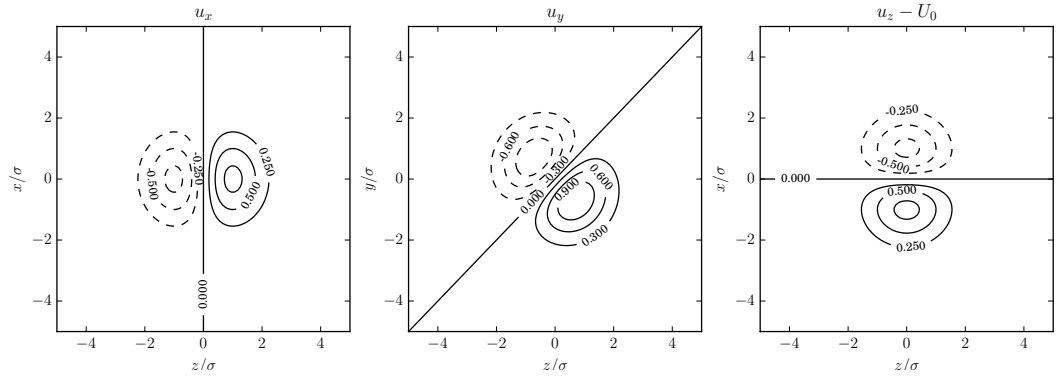

Figure 2: Contours of the components of the instantaneous velocity field at emission time $\tau = 0$ induced by a divergence-free Gaussian vortex of standard deviation σ, as defined in equation (16), convecting at Mach $M = 0.2$ along the z-axis.

Physically, this subsonic vortex should be totally silent so we seek to minimize the loading and thickness noise produced when the vortex crosses the boundary. To do so, we shall use multiple FW-H surfaces as proposed in equation (7). In this paper, we will use 4 equally spaced surfaces defined as follows. The first surface is placed at $z = 5\sigma$ so that the induced sound field is initially negligible. The subsequent surfaces are equally spaced using a separation distance Δ equal to 0.1σ, σ or 4σ. The surfaces are squares of side 10σ.

To obtain a closed FW-H surface, we enclose the origin using rectangular or square panels starting from the outlet square surfaces. However, since the velocity field induced by the vortex is very small beyond 3σ, the contributions from surfaces other than the outlet surfaces will be neglected.

Results

Figure 3 shows the time series $p(\boldsymbol{x}, t)$ in the left column, and the directivity $p_{rms}(r, \theta)$ in the right column, for the sound radiating from each of the 4 outlet surfaces. The root mean square pressure is computed simply by squaring and averaging the signal in the left column, before taking the square root. This means that the time series is periodic, with a period equal to the duration of the time series. The time series is shown for an observer at an angle $\theta = \pi/7$ from the z-axis, located in the far field at 100 wavelengths from the origin (assuming an acoustic wavelength of $f = 5$Hz). Three test cases are presented, each corresponding to a different value of the buffer thickness $D = 3\Delta$, where the separation distance Δ between two surfaces equals 8σ (top row), 2σ (middle row) and 0.2σ (bottom row), respectively.

In each figure, the result associated with the first, second, third and fourth surface are shown using square, pluses, diamonds and crosses respectvely. For the time series (left column), solid black lines obtained by interpolating the results over a finer mesh using cubic splines are added for convenience, but only the values associated with each marker have been simulated. Finally, the mean value, obtained by setting $a_i = 1/4$ in equation (7), is represented using a red dashed line.

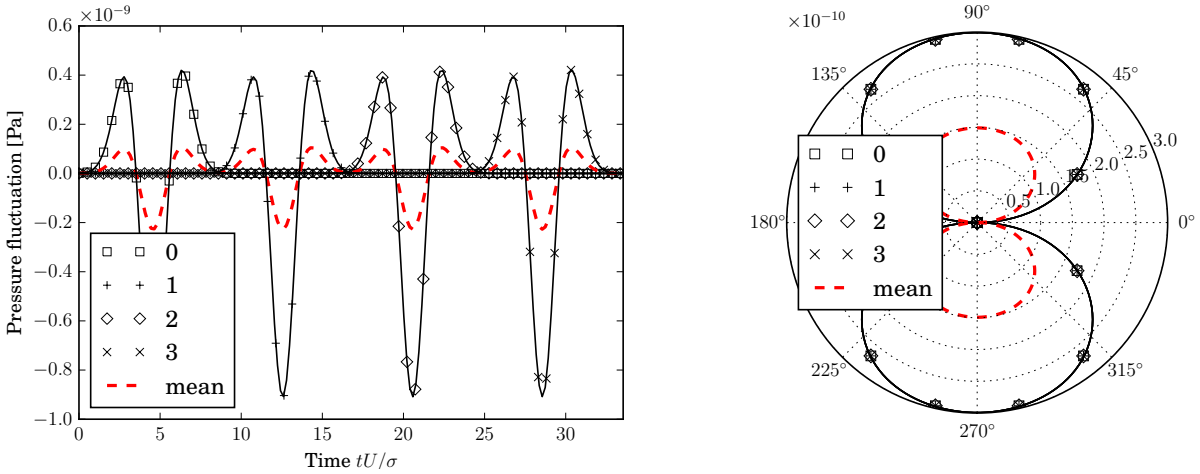

(a) Large surface separation distance $\Delta = 8\sigma$.

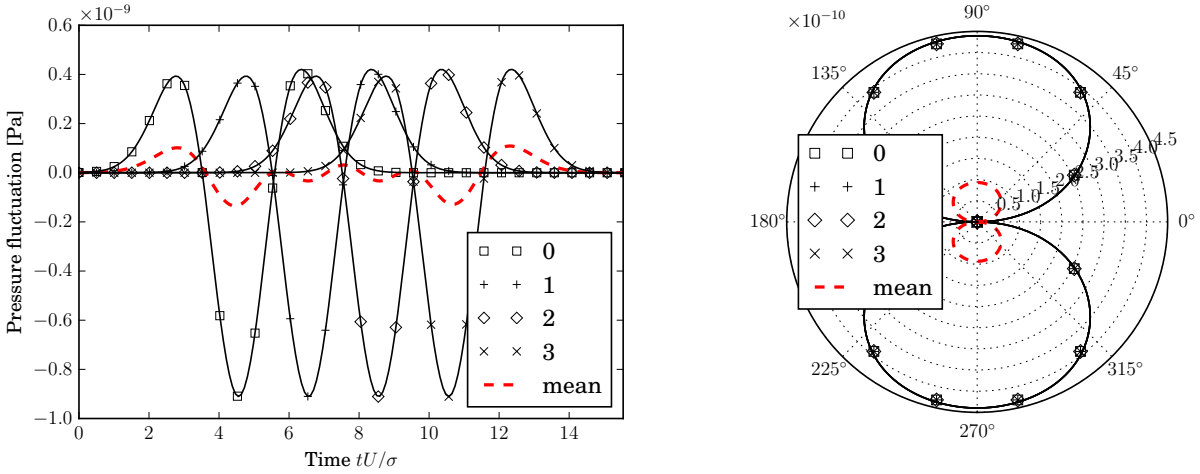

(b) Optimal surface separation distance $\Delta = 2\sigma$.

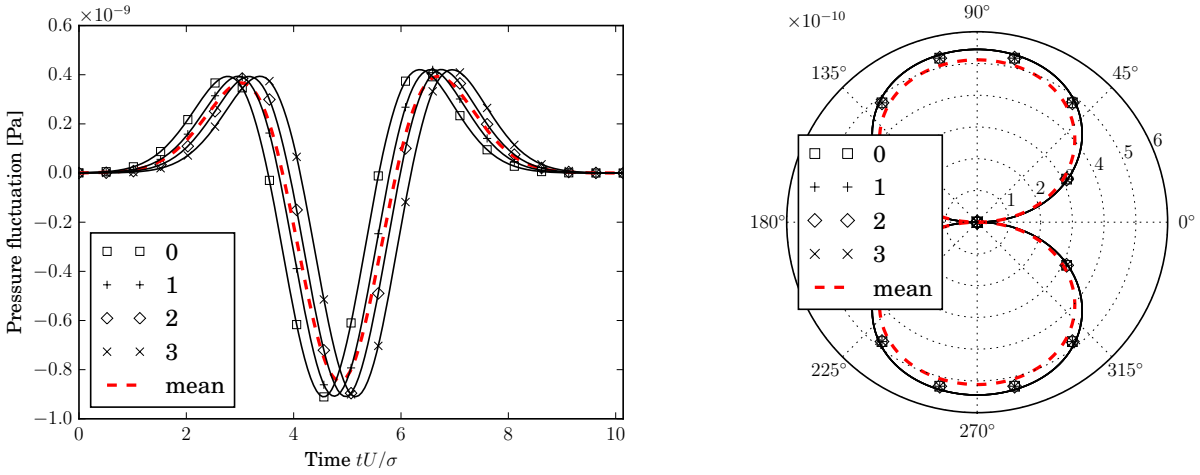

(c) Small surface separation distance $\Delta = 0.2\sigma$.

Figure 3: A Gaussian vortex of standard deviation σ convecting with the flow at Mach $M = 0.2$ and crossing 4 successive square FW-H surfaces of side 10σ, separated by a distance Δ, generates spurious noise. If Δ is large enough, averaging over the FW-H surfaces yields significant noise reduction.

Discussion

The time series in the left column of figure 3 show that the signals radiating from each of the outflow FW-H surfaces are identical but shifted in time. This is expected as the vortex is frozen and simply convects with the flow. As pointed out, for example, by Mendez et al. [5], the time lag between two FW-H surface is Δ/U. In figure 3, time is normalized by σ/U, so the normalized time lag is simply $\bar{t}_\Delta = \Delta/\sigma$.

As can be seen in the time series in figure 3(c), the impulse due to a Gaussian vortex crossing a surface lasts for rougly $\bar{T}_\sigma = 8$ (in non-dimensional time units normalized by U/σ). The signal has two peaks and one trough, located at $T_\sigma/2$.

If $\bar{t}_\Delta \ll \bar{T}_\sigma$, i.e. $\Delta \ll 8\sigma$, the time lag is small compared to the duration of the signal and there is little difference between the signals measured by each surface. This is the situation corresponding to figure 3(c). In this case, averaging the signals does not yield any substantial noise reduction.

If $\bar{t}_\Delta \geq T_\sigma$, the signals from each surface do not overlap. Averaging the signals therefore reduces the amplitude of the overall signal as $1/N$, where N is the number of surfaces. For example, in figure 3(a), where $\bar{t}_\Delta = T_\sigma$, i.e. $\Delta = 8\sigma$, the peak amplitude of the average pressure is 0.1 compared to 0.4 for the original signal (left figure) for an observer at $\pi/7$. The reduction in the sound pressure level at the peak radiation angle (near $\pi/2$) is -6 dB, and we expect it to decrease as $-\log N$.

The optimal noise reduction is obtained when the surfaces are such that the signals from neighbouring surfaces interfere with each other destructively. This can be seen in figure 3 for $\Delta = 2\sigma$, where the peak in the signal from the previous surface falls onto the trough for the signal from the current surface. The sound power is therefore minimized as illustrated in the directivity: a noise reduction of 13dB is obtained in the peak radiation angle.

In conclusion, the spurious noise from the vortical outflow can be averaged out provided that:

– the outflow buffer thickness is compact, i.e. small compared to the acoustic wavelength ($N\Delta \ll \lambda$)
– the spacing between two surfaces is larger than the vortex characteristic length, i.e. $\Delta \geq \sigma$.

For non-compact vortices, i.e. at higher frequencies, a different strategy is required. Since the buffer thickness would then become large compared to the vortex size, it may be possible to simply filter out the hydrodynamic fluctuations as proposed by Sinayoko et al. [10].

Note that it is in principle possible to obtain a better noise reduction by using coefficients a_i that are not equal to $1/N$, as suggested in Wright et al. [15]. However, for the convecting vortex case studied in this paper, the optimal set of coefficients was not found to offer much benefit over the simple arithmetic average.

4. Conclusions

This paper has investigated the generation of spurious noise due to a convecting vortex crossing the porous FW-H surface at the outflow. It was found that the noise could be reduced substantially by using an extended outflow boundary, modelled as a set of equally spaced discrete surfaces, and by computing the sound radiation from the outflow boundary by averaging the signals originating from each discrete surface. Two conditions are required to obtain significant noise reduction:

i) the distance between two surfaces must be larger than the characteristic length of the convecting vortex.
ii) the buffer thickness must be small compared to the acoustic wavelength.

The noise reduction was found to increase with the number of surfaces. For this particular test case, a simple arithmetic average was found to be nearly optimal.

More work is required to better understand how these results can be extrapolated to more complex hydrodyamic sources, in particular, whether how one can efficiently reduce spurious noise from wavepackets, or fully turbulent flow fields such as jets.

REFERENCES

1. E. J. Avital, N. D. Sandham, and K. H. Luo. Calculation of Basic Sound Radiation of Axisymmetric Jets by Direct Numerical Simulations. *AIAA Journal*, 37(2):161–168, 1999.

2. D. J. Bodony and S. K. Lele. On using large-eddy simulation for the prediction of noise from cold and heated turbulent jets. *Physics of Fluids*, 17(8):085103, 2005.

3. F. Farassat and Kenneth S. Brentner. The Acoustic Analogy and the Prediction of the Noise of Rotating Blades. *Theoretical and Computational Fluid Dynamics*, 10(1-4):155–170, January 1998.

4. T. Ikeda, S. Enomoto, K. Yamamoto, and K. Amemiya. On the Modification of the Ffowcs Williams-Hawkings Integration for Jet Noise Prediction. In *19th AIAA/CEAS Aeroacoustics Conference*. American Institute of Aeronautics and Astronautics, 2013.

5. S. Mendez, M. Shoeybi, S. K. Lele, and P. Moin. On the use of the Ffowcs Williams-Hawkings equation to predict far-field jet noise from large-eddy simulations. *International Journal of Aeroacoustics*, 12(1):1–20, June 2013.

6. A. Najafi-Yazdi, G. A. Bres, and L. Mongeau. An acoustic analogy formulation for moving sources in uniformly moving media. *Proceedings of the Royal Society A: Mathematical, Physical and Engineering Sciences*, 467(2125):144–165, 2010.

7. Zane Nitzkorski and Krishnan Mahesh. A dynamic end cap technique for sound computation using the Ffowcs Williams and Hawkings equations. *Physics of Fluids (1994-present)*, 26(11):115101, November 2014.

8. A. Sescu and R. Hixon. Toward low-noise synthetic turbulent inflow conditions for aeroacoustic calculations. *International Journal for Numerical Methods in Fluids*, 73(12):1001–1010, 2013.

9. M. Shur, P. R. Spalart, and M. Strelets. Noise prediction for increasingly complex jets. Part I: Methods and tests. *International Journal of Aeroacoustics*, 4(3):213–246, July 2005.

10. S. Sinayoko, A. Agarwal, and Z. Hu. Flow decomposition and aerodynamic sound generation. *Journal of Fluid Mechanics*, 668(2005):335–350, December 2010.

11. P. R. Spalart and M. L. Shur. Variants of the Ffowcs Williams-Hawkings equation and their coupling with simulations of hot jets. *International journal of aeroacoustics*, 8(5):477–491, 2009.

12. M. Wang, S. K. Lele, and P. Moin. Computation of quadrupole noise using acoustic analogy. *AIAA Journal*, 34(11):2247–2254, 1996.

13. J. E. Ffowcs Williams and D. L. Hawkings. Sound Generation by Turbulence and Surfaces in Arbitrary Motion. *Philosophical Transactions of the Royal Society of London. Series A, Mathematical and Physical Sciences*, 264(1151):321–342, May 1969.

14. W. R. Wolf and S. K. Lele. Trailing-Edge Noise Predictions Using Compressible Large-Eddy Simulation and Acoustic Analogy. *AIAA Journal*, 50(11):2423–2434, November 2012.

15. Wright, M. C. M. and Morfey, C. L. On the extrapolation of acoustic waves from flow simulations with vortical outflow. *International Journal of Aeroacoustics*, 14(1-2):217–227, 2015.